

**DEDICATION**

**ACKNOWLEDGEMENTS**

**CONTENTS**

**LIST OF FIGURES**

**LIST OF TABLES**

**LIST OF ACRONYMS**

CHAPTER I

**Introduction**

1.1 Major issues of the study on CdSe nanocrystals. . . . .	1
1.2 Wurtzite and zinc-blende structure. . . . .	3
1.3 Electronic structure of CdSe nanocrystals. . . . .	7
1.4 Framework of the thesis. . . . .	12
1.5 References. . . . .	14

CHAPTER II

**Experimental Principles and Approaches**

2.1 Preparation of CdSe nanocrystals by colloidal method. . .	18
2.2 TEM and optical characterization. . . . .	20
2.3 X-ray diffraction. . . . .	23
2.4 X-ray absorption spectroscopy. . . . .	29
2.5 Photoemission spectroscopy. . . . .	40
2.6 References. . . . .	46

## CHAPTER III

### **Size Dependence of Structural Characteristics in CdSe Nanocrystals**

3.1 Introduction. . . . .	49
3.2 Simulation of X-ray diffraction patterns. . . . .	50
3.3 Diffraction patterns fitted with a simple model. . . . .	56
3.4 EXAFS studies on bond lengths. . . . .	60
3.5 Discussion. . . . .	72
3.6 Summary. . . . .	79
3.7 References. . . . .	79

## CHAPTER IV

### **Photoemission Final-State Effect on Electronic Properties of CdSe Nanocrystals**

4.1 Introduction. . . . .	83
4.2 Size dependence of photoemission spectra. . . . .	84
4.3 Photoemission final-state effect. . . . .	91
4.4 Discussion. . . . .	92
4.5 Summary. . . . .	104
4.6 References. . . . .	104

## CHAPTER V

### **Relation between Surface Properties and Photoluminescence Efficiency in CdSe Nanocrystals**

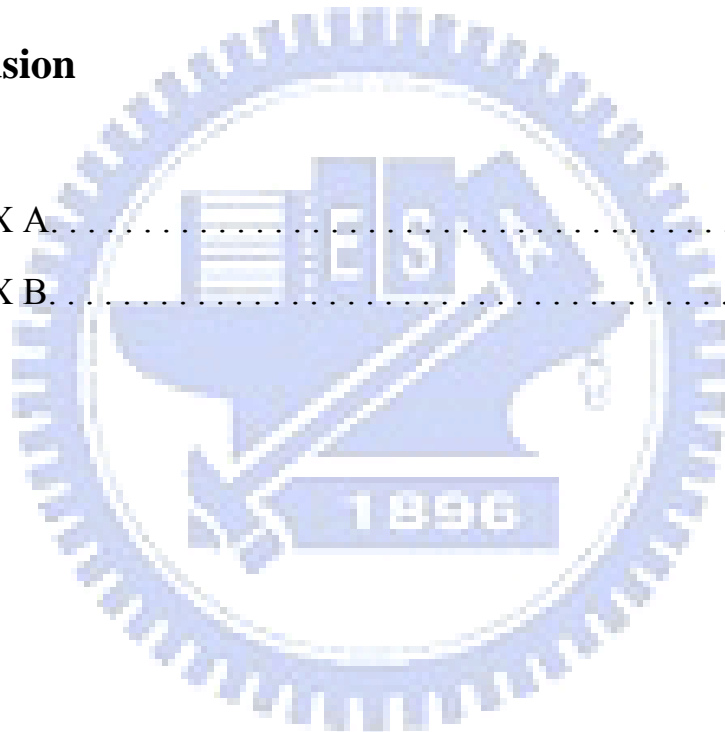
5.1 Introduction. . . . .	106
---------------------------	-----

5.2 Growth rate. . . . .	108
5.3 Absorption and photoluminescence measurements. . . . .	109
5.4 Photoemission studies. . . . .	111
5.5 Discussion. . . . .	117
5.6 Summary. . . . .	120
5.7 References. . . . .	120

CHAPTER VI

**Conclusion**

APPENDIX A. . . . .	126
APPENDIX B. . . . .	129



## LIST OF FIGURES

### Figure

<b>1.1:</b> The scheme of a unit cell of wurzite structure. . . . .	4
<b>1.2:</b> Crystal structure of zinc-blende structure and atomic positions. . . . .	5
<b>1.3:</b> Three views of the wurzite and zinc-blende crystal structures. . . . .	6
<b>1.4:</b> Absorption spectrum of CdSe nanoparticles with size of 33 Å. . . . .	8
<b>1.5:</b> Lowest transition energy of CdSe nanoparticles as a function of size. . . . .	9
<b>2.1:</b> The schematic representation of the organometallic preparation of CdSe NCs using TOPO, HDA, and TOP. . . . .	19
<b>2.2:</b> TEM images of CdSe nanocrystals passivated with TOPO/HDA and treated by pyridine. . . . .	20
<b>2.3:</b> Size histograms of CdSe NCs. . . . .	21
<b>2.4:</b> Optical spectra of CdSe nanocrystals. . . . .	22
<b>2.5:</b> Color photograph for different size samples of CdSe nanocrystals. . . . .	23
<b>2.6:</b> Relations involved in letting the $r_{mn}$ vector take all orientations in space. . . . .	27
<b>2.7:</b> Schematic representation of X-ray diffraction apparatus used in conventional mode. . . . .	28
<b>2.8:</b> The brilliance of X-ray sources as a function of time. . . . .	29
<b>2.9:</b> Schematic representation of the accelerator and experimental facilities at the NSRRC, the Taiwan Light Source. . . . .	30
<b>2.10:</b> The bright spectra from NSRRC light sources, compared to traditional light sources. . . . .	31
<b>2.11:</b> X-ray absorption measurements. . . . .	33
<b>2.12:</b> The absorption cross-section $\mu/\rho$ for Cd and Se over the x-ray energy range of 1 to 100 keV. . . . .	34
<b>2.13:</b> Schematic representation of the set-up for EXAFS measurements using synchrotron radiation. . . . .	36
<b>2.14:</b> Se <i>K</i> -edge EXAFS spectrum of bulk CdSe. . . . .	37
<b>2.15:</b> Schemes of scattering processes. . . . .	38
<b>2.16:</b> Se <i>K</i> -edge EXAFS <i>k</i> - and <i>k</i> <sup>3</sup> -weighted spectra of bulk CdSe. . . . .	39
<b>2.17:</b> Energy diagram of the photoemission process. . . . .	43

<b>2.18:</b> Synchrotron photoemission spectrum of CdSe nanocrystals passivated with TOPO/HDA. . . . .	44
<b>2.19:</b> Schematic diagram of photoemission experiment. . . . .	46
<b>3.1:</b> Powder X-ray diffraction spectra of bulk CdSe and CdSe NC. . . . .	51
<b>3.2:</b> Powder diffraction pattern of TOPO/HDA-passivated CdSe NCs and the calculated patterns for wurtzite and zinc-blende NCs with size of 31 Å. . . . .	54
<b>3.3:</b> Experimental diffraction spectra of bulk CdSe and three CdSe NCs as well as the corresponding simulations by Debye formula. . . . .	55
<b>3.4:</b> The wurtzite stacking fraction as a function of the NC mean diameter. . . . .	56
<b>3.5:</b> Powder X-ray diffraction patterns of CdSe NCs and the corresponding fits. . . . .	59
<b>3.6:</b> Size-dependent lattice parameters of CdSe NCs determined by fit of powder XRD data. . . . .	60
<b>3.7:</b> $k^3$ -weighted Cd and Se <i>K</i> -edge EXAFS spectra of bulk CdSe and NCs. . . . .	61
<b>3.8:</b> Fourier transforms of Cd and Se <i>K</i> -edge EXAFS spectra for bulk CdSe and three-sized nanocrystals. . . . .	62
<b>3.9:</b> Fourier filtered EXAFS spectra and the best fits of CdSe NCs. . . . .	64
<b>3.10:</b> Fourier transforms of Se <i>K</i> -edge EXAFS spectra, measured at ~10 K, for CdSe NCs with mean diameter 31 Å. . . . .	65
<b>3.11:</b> The measured first-shell coordination numbers of five NCs are plotted with the calculated values by the ball-and-stick model. . . . .	67
<b>3.12:</b> Mean length of the Cd–Se and Cd–O/N bonds for CdSe nanocrystals. . . . .	68
<b>3.13:</b> The scheme of a tetrahedral structure. . . . .	69
<b>3.14:</b> Single-shell filtered Se <i>K</i> -edge data measured at the temperature of ~10 K and the corresponding fits. . . . .	70
<b>3.15:</b> Size dependence of normalized bond lengths, $R^{(1)}$ and $R^{(2)}$ , for CdSe NCs passivated with TOPO/HDA is plotted together with the normalized lattice parameters, $c$ and $a$ . . . . .	71
<b>3.16:</b> The structural parameters $u$ of CdSe nanocrystals. . . . .	72
<b>3.17:</b> Relative structure parameters of CdSe NCs dependent on particle size. . . . .	74
<b>3.18:</b> Surface energy of TOPO/HDA-passivated CdSe NCs as a function of size. . . . .	76
<b>3.19:</b> Schematic diagram of the size-dependent phase transition of CdSe. . . . .	78
<b>4.1:</b> Size-dependent Cd $3d_{5/2}$ and Se $3d$ photoemission spectra of bulk CdSe and	

TOPO/HDA-passivated CdSe nanocrystals. . . . .	.85
<b>4.2:</b> Valence-band photoemission spectra of bulk CdSe and TOPO/HDA-passivated CdSe nanocrystals. . . . .	.87
<b>4.3:</b> P $2p$ photoemission spectra of CdSe nanocrystals passivated with TOPO/HDA and treated with pyridine. . . . .	.88
<b>4.4:</b> Core-level photoemission spectra of bulk CdSe and CdSe nanocrystals passivated with TOPO/HDA and treated with pyridine. . . . .	.89
<b>4.5:</b> Photoemission spectra in the valence-band binding-energy regime of bulk CdSe and CdSe nanocrystals passivated with TOPO/HDA and treated with pyridine. . . . .	.90
<b>4.6:</b> Energy shifts of the core levels and the valence-band edge for TOPO/HDA-passivated CdSe nanocrystals compared with model calculations. . . . .	.95
<b>4.7:</b> Schematic diagram of the dynamic final-state effect. . . . .	.99
<b>4.8:</b> Energy shifts of the core levels and the valence-band edge for CdSe nanocrystals treated with pyridine compared with model calculations. . . . .	100
<b>5.1:</b> The NC size as a function of evolution time during growth for NCs prepared using OPA and those using OA. . . . .	109
<b>5.2:</b> Room temperature optical absorption and PL spectra of OA-prepared CdSe NCs dispersed in toluene. . . . .	110
<b>5.3:</b> The normalized PL intensity as a function of NC diameter for OPA- and OA-prepared NCs. . . . .	111
<b>5.4:</b> Fits to the Cd $3d_{5/2}$ core-level photoemission spectra of OA prepared CdSe nanocrystals. . . . .	112
<b>5.5:</b> Fits to the Se $3d$ core-level photoemission spectra of OA-prepared CdSe nanocrystals. . . . .	114
<b>5.6:</b> The ratio of the surface component to total intensity determined from the Se $3d$ photoemission spectra of CdSe NCs prepared using OPA and OA. . . . .	117
<b>5.7:</b> The normalized PL intensity and number of the unpassivated surface Se atoms for OPA- and OA-prepared NPs. . . . .	118
<b>5.8:</b> The normalized PL intensity as a function of the number of the unpassivated surface Se atoms for CdSe NCs prepared using OPA and OA. . . . .	119
<b>A.1:</b> An ellipsoidal particle represents in real and reciprocal space. . . . .	127
<b>B.1:</b> The representation of a charge $q$ inside a dielectric sphere. . . . .	130

## LIST OF TABLES

### Table

<b>1.1</b> Structural parameters of CdSe and ideal wurtzite. . . . .	4
<b>3.1</b> Structural parameters derived from EXAFS spectra of CdSe nanocrystals. . . . .	65



## LIST OF ACRONYMS

DW factor.....	Debye-Waller factor
ESCA.....	electron spectroscopy for chemical analysis
EXAFS.....	extended X-ray absorption fine structure
HDA.....	hexadecylamine
IMFP.....	inelastic mean free path
KT.....	Koopman's theorem
NCs.....	nanocrystals
OA.....	oleic acid
OPA.....	octadecylphosphonic acid
PES.....	photoemission/photoelectron spectroscopy
PL.....	photoluminescence
QDs.....	quantum dots
TEM.....	transmission electron microscope
TOP.....	trioctylphosphine
TOPO.....	trioctylphosphine oxide
UV.....	ultraviolet
WZ.....	wurtzite
XANES.....	X-ray absorption near-edge spectroscopy
XRD.....	X-ray diffraction
ZB.....	zinc blende